

Optogenetic Inhibition of the Subthalamic Nucleus Reduces Levodopa-Induced Dyskinesias in a Rat Model of Parkinson's Disease

Hyung Ho Yoon^a Joongkee Min^a Eunmi Hwang^b C. Justin Lee^b
Jun-Kyo Francis Suh^c Onyou Hwang^d Sang Ryong Jeon^a

^aDepartment of Neurological Surgery, Asan Medical Center, University of Ulsan College of Medicine, ^bCenter for Neural Science and WCI Center for Functional Connectomics, Korea Institute of Science and Technology, ^cCenter for Bionics of Korea Institute of Science and Technology, and ^dDepartment of Biochemistry and Molecular Biology, University of Ulsan College of Medicine, Seoul, Republic of Korea

Key Words

Deep brain stimulation · Halorhodopsin · Levodopa-induced dyskinesia · Optogenetics · Subthalamic nucleus

Abstract

Background: The inhibition of neuronal activity by electrical deep brain stimulation is one of the mechanisms explaining the amelioration of levodopa-induced dyskinesia. However, electrical deep brain stimulation cannot specifically activate or inactivate selected types of neurons. **Objectives:** We applied optogenetics as an alternative treatment to deep brain stimulation for levodopa-induced dyskinesia, and also to confirm that the mechanism of levodopa-induced dyskinesia amelioration by subthalamic nucleus deep brain stimulation is mediated through neuronal inhibition. **Methods:** 6-hydroxydopamine-induced hemiparkinsonian rats received injections of hSynapsin1-NpHR-YFP adeno-associated virus (AAV) or hSynapsin1-YFP AAV. Two weeks after viral injections, all rats were treated with daily injections of levodopa. Then, the optic fiber was implanted into the ipsilateral subthalamic nucleus. We performed various behavioral tests to evaluate the changes in levodopa-induced dys-

kinesias after optogenetic expression and illumination in the subthalamic nucleus. **Results:** The behavioral tests revealed that optical inhibition of the subthalamic nucleus significantly ameliorated levodopa-induced dyskinesia by reducing the duration of the dyskinesias as well as the severity of axial dyskinesia. **Conclusions:** These findings will provide a useful foundation for the future development of optogenetic modulation systems that could be considered as an approach to dyskinesia therapy.

© 2016 S. Karger AG, Basel

Introduction

Parkinson's disease, the second most common neurodegenerative disease, is characterized by dopaminergic depletion in the nigrostriatal pathway leading to motor symptoms such as tremor, rigidity, and bradykinesia [1, 2]. The dopamine precursor L-3,4-dihydroxyphenylalanine (L-DOPA) has been largely used as a treatment in patients with Parkinson's disease since the 1960s [2]. However, the long-term use of L-DOPA may induce dyskinesias, wearing off, and motor fluctuations [3]. Deep

brain stimulation (DBS) surgery was proposed for patients with advanced Parkinson's disease to reduce these complications [4, 5]. However, it is still unclear whether the mechanisms underlying the positive effects following DBS is from electrical stimulation that inhibits or activates target neurons [6, 7]. In addition, it is difficult to stimulate a specific neuron because of the nature of this nonspecific electrical stimulation [8]. A new technology using optogenetics and illumination was developed that allows for the modulation of specific neurons [9, 10]. Chloride pump halorhodopsin can be transfected using adeno-associated virus (AAV) in the target region when illuminated with yellow light (wavelength, 590 nm), resulting in hyperpolarization and inhibition from firing action potential [11]. Recently, we provided evidence that optogenetic subthalamic nucleus (STN) inactivation improves the akinesia observed in a rat model of Parkinson's disease [12]. In the present study, we applied optogenetics to the treatment of levodopa-induced dyskinesia (LID), which is another treatment target of DBS.

In parkinsonism, the deficiency in dopamine release leads to a disinhibition of the indirect pathway, resulting in reduced neural activity in the external segment of the globus pallidus, followed by an increase in neural activity in the STN [13, 14]. Abnormal neural activity in the STN is related to excessive and uncontrollable movements [15]. However, L-DOPA treatment in the 6-hydroxydopamine (6-OHDA)-induced rat model of Parkinson's disease did not modulate the hyperactivity observed in the STN [13]. Thus, another goal of the present study was to clarify the therapeutic mechanism of STN DBS on LID.

In this study, we investigated the effects of optical inhibition in the STN using the expression and illumination of halorhodopsin in a rat model of Parkinson's disease with LID. It was assessed using abnormal involuntary movement (AIM) scores, stepping tests, and cylinder tests.

Materials and Methods

Experimental Animals

Male Wistar rats (Orient Bio Inc., Seongnam, Korea), weighing 250–300 g at the beginning of the experiment, were housed in a room with a 12-hour light/dark cycle and had free access to food and water. All procedures complied with the guidelines of the Institutional Animal Care and Use Committee of the Asian Institute for Life Sciences (Seoul, Korea).

Experimental Design

The timeline of the experiments is presented in figure 1. Three weeks after 6-OHDA injections, all rats were separated into three

groups. The NpHR+590nm group was an experimental group, with each rat subjected to a virus injection, optic fiber insertion, and 590 nm of light illumination. The NpHR+Sham group was a control, with a lesion created by the optic fiber, and each rat in this group was also subjected to a virus injection and optic fiber insertion but no light illumination. The YFP+590nm group was a control for the light illumination, with each rat subjected to a control virus injection, optic fiber insertion, and 590 nm of light illumination. The NpHR+590nm group (n = 9) and NpHR+Sham group (n = 7) received hSynapsin1-NpHR-yellow fluorescent protein (YFP) AAV injections that were targeted to the right hemisphere STN. The YFP+590nm group (n = 7) received hSynapsin1-YFP AAV injections. Two weeks after viral injections, all rats were treated with daily injections of L-DOPA (6 mg/kg; Sigma, St. Louis, Mo., USA) and benserazide (15 mg/kg; Sigma) until all experiments were completed. Twenty days after the first injection of L-DOPA, the optic fiber was implanted into the ipsilateral STN. Then, rats in the NpHR+590nm and YFP+590nm groups received 590 nm of light illumination during behavioral tests. The 6-OHDA-lesioned rats (23 of 29 rats) that showed net contralateral rotations at a rate greater than 6/min during the apomorphine-induced rotation test were selected for inclusion. However, 2 of the 23 selected animals showed little or no response to L-DOPA and were excluded from the AIM scoring.

6-OHDA Lesion Surgery

Surgical procedures were performed under general anesthesia induced by an intraperitoneal injection of a mixture of 35 mg/kg zolazepam and tiletamine (Zoletil; Virbac S.A., Carros, France) and 5 mg/kg xylazine (Rompun; Bayer, Leverkusen, Germany). A total of 29 rats received unilateral injections of 8 μ g of 6-OHDA (Sigma, St. Louis, Mo., USA) in 4 μ l of 0.9% saline with 0.1% ascorbic acid into the right medial forebrain bundle at the coordinates AP -2.2 mm, L +1.5 mm relative to bregma, and V -8.0 mm from the dura, with the tooth bar set at +4.5 mm [16]. The toxin was delivered at a rate of 1 μ l/min using a 33-gauge Hamilton syringe and an automated microsyringe pump (Harvard Apparatus, Holliston, Mass., USA). After injection, the needle was kept in place for 5 min to prevent the solution from flowing backward and was then retracted over a subsequent 5 min.

Rotation Screening for the Parkinson's Disease Model

The apomorphine-induced rotation test was performed 1 week after 6-OHDA injection. Briefly, apomorphine (0.25 mg/kg; Sigma) in sterile water was subcutaneously administered, and the rat was immediately harnessed to an automated rotameter (Panlab, Barcelona, Spain). Ipsi- and contralateral rotations were recorded for 45 min. The data were expressed as the net (contralateral - ipsilateral turns) average rotations/min (data not shown). Rats that had >6 contralateral rotations/min were selected for the study.

Preparation of hSynapsin1-NpHR-YFP AAV and hSynapsin1-YFP AAV

The AAV vector plasmid pAAV2-hSynapsin1-NpHR-YFP was constructed by removing the CMV promoter from pAAV2-CMV (Stratagene, La Jolla, Calif., USA) and inserting the hSynapsin1 promoter and NpHR-YFP sequence (plasmid No. 26775, Addgene). The pAAV2-hSynapsin1-YFP AAV was used as a control vector with only the YFP sequence instead of the NpHR-YFP sequence. The pAAV-RC plasmid harbors the AAV rep and cap

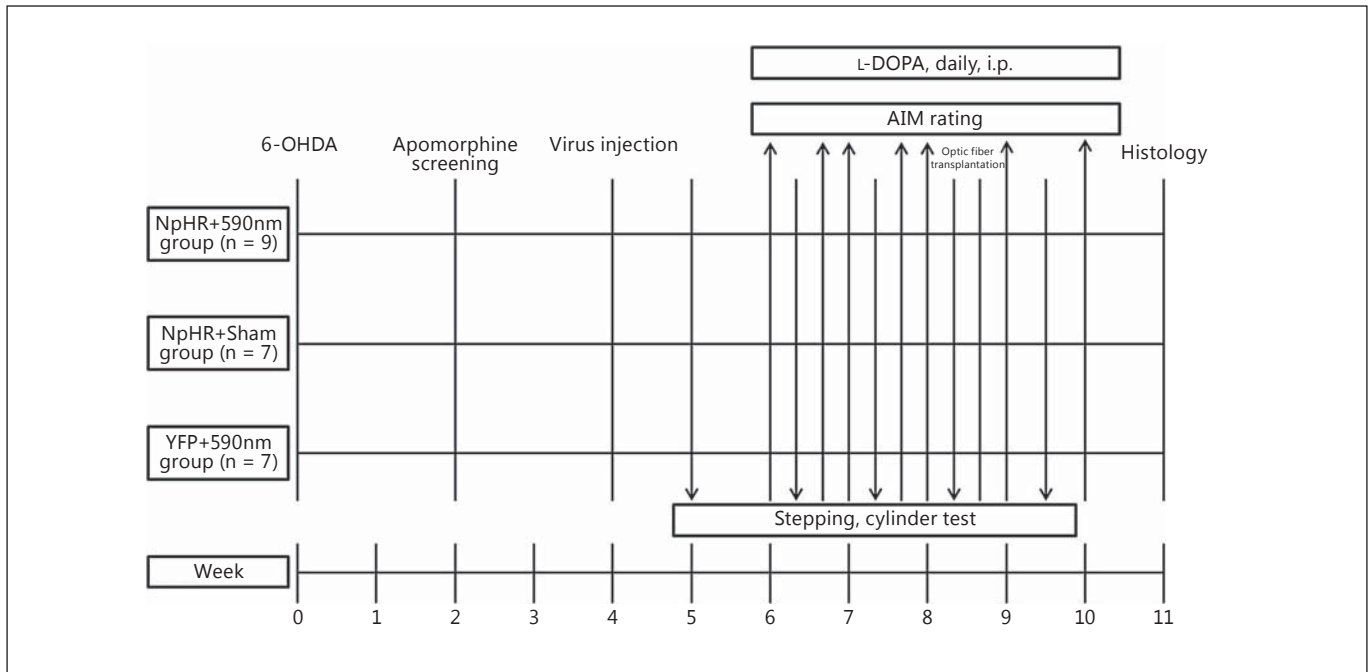


Fig. 1. Timeline of the experiments. Three weeks after 6-OHDA injections, all rats were separated into three groups. The NpHR±590nm group was an experimental group, with each rat subjected to a virus injection, optic fiber insertion, and 590 nm of light illumination. The NpHR±Sham group was a control, with a

lesion created by the optic fiber, and each rat in this group was also subjected to a virus injection and optic fiber insertion, but no light illumination. The YFP±590nm group was a control for the light illumination, with each rat subjected to a control virus injection, optic fiber insertion, and 590 nm of light illumination.

genes encoding the replication and virus capsid structure protein, respectively. The pHelper plasmid contains the essential subset of adenovirus genes, VA, E2A, and E4, necessary for AAV production in HEK293 cells. For AAV2/2 production, three AAV plasmids (10 µg of each plasmid) were cotransfected into HEK293 cells using a polyethylenimine transfection kit (Polyplus, Illkirch-Graffenstaden, France).

Stereotactic AAV Injection

The number of viral particles was a minimum of 1.0×10^{10} /ml, which is considered a concentrated virus package. Three weeks after injection of 6-OHDA, viral injections were performed under general anesthesia induced by an intraperitoneal injection of a mixture of 35 mg/kg of Zoletil and 5 mg/kg of Rompun. The NpHR+590nm group (n = 9) and the NpHR+Sham group (n = 7) received injections of hSynapsin1-NpHR-YFP AAV (2.0 µl) that targeted the ipsilateral STN (coordinates: AP -3.8 mm, L +2.5 mm relative to bregma, and V -7.8 mm from the dura)[17], and the YFP+590nm group (n = 7) received an equivalent volume injection of hSynapsin1-YFP AAV. The AAV were delivered at a rate of 0.2 µl/min using a Hamilton syringe and an automated microsyringe pump in the same manner as that for the 6-OHDA injection.

Optic Fiber Implantation and Light Stimulation

Optic fibers (200-µm core, 245-µm outer diameter, numerical aperture 0.53, RM3 type, flat tip; Doric Lenses, Québec City, Qué.,

Canada) were cut to the length of 8.5 mm for optimizing to the depth of the STN. Twenty days after the first injection of L-DOPA, each rat was positioned in a stereotactic frame under general anesthesia. After a scalp incision, four burr holes were drilled to embed screws around the insertion site of the optic fiber. The optic fiber was implanted using a stereotactic cannula holder into the STN that was the same site of the AAV injection. The optic fiber was firmly fixed with surrounding screws using dental cement (Vertex, Zeist, The Netherlands). For light illumination, the implanted optic fiber was connected to a fiber-optic rotary joint and an LED fiber-optic light source (Doric Lenses) that produced amber (590 nm) light. A frequency of 5 Hz was applied under the control of a function generator (EZ Digital, Bucheon, Korea) with a TTL signal. The light was illuminated in freely moving animals during the AIM ratings, stepping tests, and cylinder tests.

AIM Rating

Two weeks after viral injections, LID was induced using daily injections of L-DOPA (6 mg/kg, i.p.) in 0.9% saline. The DOPA decarboxylase inhibitor benserazide (15 mg/kg, i.p.) was injected 20 min prior to L-DOPA injection for efficient transport of L-DOPA into the brain [18]. AIMS were scored according to the rat dyskinesia scale as previously described [19, 20] with slight modifications. Briefly, after the L-DOPA injection, each rat was individually placed into a transparent plastic cage, and the AIMS were scored once every 20 min for 120 min. The AIMS were classified into three subtypes of dyskinesia: limb, axial, and orolingual. Limb

and orolingual dyskinesias were scored from 0 to 4: 0 = absent, 1 = present during less than 50% of the observation time, 2 = present during more than 50% of the observation time, 3 = present continuously, interrupted by stimuli, and 4 = present continuously, not interrupted by stimuli. Axial dyskinesia was scored from 0 to 4: 0 = absent, 1 = contralateral flexion of head, 2 = contralateral flexion of neck and upper body, 3 = contralateral flexion of neck and upper body toward upper tail, and 4 = contralateral flexion of neck and upper body toward upper tail and falling down. The AIMs were evaluated seven times at a frequency of twice per week: five times before optic fiber implantation and two times after optic fiber implantation under light illumination (590 nm). The AIMs were rated by investigators blinded to the experiment and familiar with the dyskinesia rating scales, and then data were summed by another blinded investigator. The optogenetic probe in this study cannot be visualized regardless of whether it is on or off because the light-connected ferrule is concealed in the probe system, so the blinded investigator did not recognize whether the light was on or off.

Stepping Test

The stepping test was performed five times: prior to the L-DOPA injection (PD), once per week during the L-DOPA injections (LID1, LID2, and LID3), and once during an L-DOPA injection under light illumination (LIGHT). Each stepping test was performed 100 min after the L-DOPA injection. The stepping test was performed as previously described with slight modifications [12, 21]. Briefly, both hind limbs were firmly held in one hand of the experimenter, while one of the forelimbs was held in the other hand. The test was repeated with both the contralateral and ipsilateral forelimbs. The rostral part of the rat was lowered onto a treadmill (Jeung Do Bio & Plant Co., Seoul, Korea) that was moving at a rate of 1.8 m/10 s. The rat's body remained stationary while one forelimb was allowed to spontaneously touch the moving treadmill track for 10 s. All experimental sessions were video recorded to allow the number of adjusted steps taken in the forehand, backhand, and backward direction to be counted. Every rat performed the stepping test twice in each session, and the number of steps taken was averaged across the two trials. Data are expressed as the number of forelimb touches.

Cylinder Test

The cylinder test was performed five times: before the L-DOPA injection (PD), once per week during L-DOPA injections (LID1, LID2, and LID3), and once during an L-DOPA injection under conditions of light illumination (LIGHT). Each cylinder test was performed 60–70 min after the L-DOPA injection as previously described [12, 22]. Briefly, a rat was placed in a transparent glass cylinder (diameter: 20 cm; height: 35 cm) until the animal explored the walls vertically with his forelimbs more than 20 times. All the tests were recorded to count the number of spontaneous wall contacts. The first 20 wall contacts were included for data analysis and are expressed as the percentage of contralateral forelimb contacts. When the rats used both forelimbs symmetrically, the contralateral forelimb touch rate was 50%.

Tissue Processing

For tissue fixation, rats were transcardially perfused with 0.9% saline containing 10,000 IU heparin (Hanlim Pharm, Seoul, Korea), followed by 4% paraformaldehyde in phosphate-buffered sa-

line (PBS). Brains were extracted and postfixed overnight in the same fixative, followed by dehydration in 30% sucrose until they sank. Coronal sections (40- μ m thick) of the STN (AP: -3.36 to -4.08 mm) and the substantia nigra (SN; AP: -4.8 to -6.0 mm) were collected using a cryotome (Thermo Scientific, Waltham, Mass., USA) and preserved under free-floating conditions in 0.08% sodium azide (Sigma) in PBS at 4°C.

Histology

Immunostaining and immunofluorescence procedures were performed as previously described [23]. Serial coronal sections of the STN were washed in 0.5% bovine serum albumin (BSA; Bioworld, Dublin, Ohio, USA) in PBS (pH 7.4) and incubated with a blocking solution containing BSA, Triton X-100 (Sigma), and sodium azide (Sigma) in PBS. The STN sections were incubated overnight with a rabbit anti-vesicular glutamate transporter 2 antibody (VGLUT2; 1:300; Synaptic Systems, Göttingen, Germany) in 0.5% BSA in PBS. They were subsequently incubated for 2 h with Alexa Fluor 555 goat anti-rabbit IgG (1:1,000; Invitrogen, Carlsbad, Calif., USA). Fluorescent-labeled tissues were coverslipped with fluorescent mounting medium (Dako, Glostrup, Denmark). The SN sections (rostral section: -4.8 mm; medial section: -5.4 mm; caudal section: -6.0 mm) were selected and incubated overnight with a mouse anti-tyrosine hydroxylase antibody [1:2,000; tyrosine hydroxylase (TH); Sigma] in 0.5% BSA in PBS (pH 7.4). They were subsequently incubated for 2 h with biotinylated anti-mouse IgG (1:200; Vector Laboratories, Burlingame, Calif., USA) in the same solution. The complexes of primary and secondary antibodies were visualized using the diaminobenzidine (R&D Systems, Minneapolis, Minn., USA) colorimetric reaction.

Imaging and Nigral Cell Counting

Fluorescent images were obtained using a confocal microscope (Carl Zeiss, Oberkochen, Germany) with ZEN microscope software (Carl Zeiss). For nigral cell counting, TH-immunopositive cells on both sides of the SN were observed in three coronal sections using a Nikon 80i microscope (Nikon, Tokyo, Japan) with NIS-Elements F3.0 software at 100 \times magnification. Data are expressed as the percentage of cell loss in the ipsilateral SN compared with the number of cells in the contralateral SN.

Statistical Analysis

All data are presented as means \pm SD. All statistical analyses were performed using SPSS (version 21; IBM, Armonk, N.Y., USA). A repeated-measures ANOVA was conducted to analyze differences in the time-dependent patterns of the AIM scores. AIM scores were analyzed using paired t tests. Stepping tests and cylinder tests were analyzed using a one-way ANOVA with Tukey's post hoc test.

Results

Effect of Optical Inhibition of STN on LID

Before optic fiber implantation, the AIM scores showed a plateau or a slight increase during LID4 and LID5 sessions in each group (fig. 2). After optic fiber implantation,

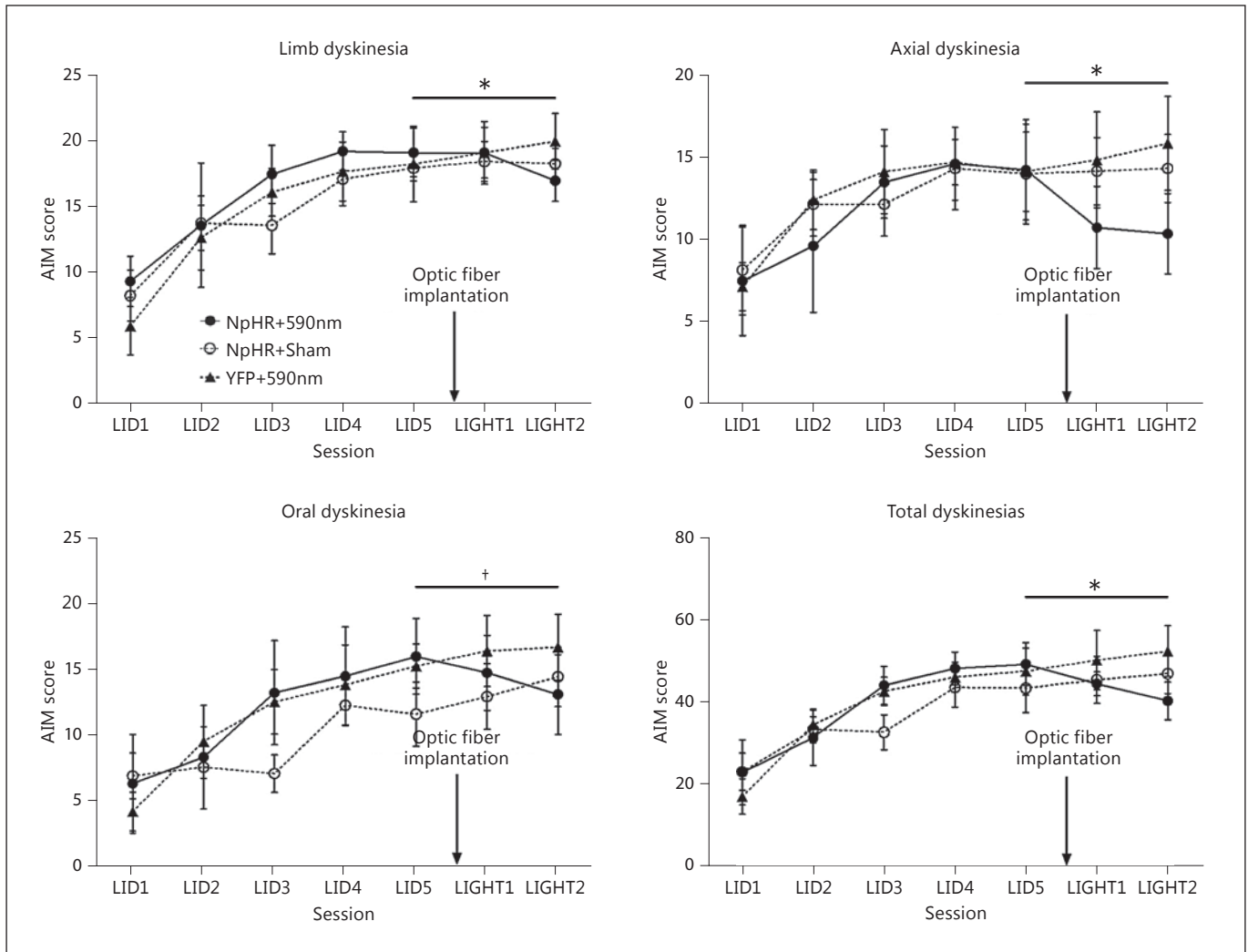


Fig. 2. Optical inhibition of the STN affects the time-dependent patterns of LID. The AIMs were evaluated twice per week for a total of seven evaluations: five times before optic fiber implantation and two times after optic fiber implantation under light illumination (590 nm). The AIMs were classified into three subtypes: limb, axial, and orolingual dyskinesia. The time-dependent patterns of

AIM scores during the LID5, LIGHT1, and LIGHT2 sessions show a decrease in the NpHR+590nm group, whereas they show a continuous increase in the NpHR+Sham and YFP+590nm groups. Data are expressed as means \pm SD. * $p < 0.001$, † $p = 0.001$; repeated measures ANOVA.

the AIMs were scored under 590 nm of light illumination, except the NpHR+Sham group. The pattern of AIM scores during the LID5, LIGHT1, and LIGHT2 sessions showed a decrease in the NpHR+590nm group, whereas they plateaued or continuously increased in the NpHR+Sham and YFP+590nm groups. There were significant differences in the time-dependent patterns among the groups: limb dyskinesia ($p < 0.001$, $F = 7.281$, $d.f. = 3.804$), axial dyskinesia ($p < 0.001$, $F = 8.475$, $d.f. = 2.959$), oral dyskinesia ($p = 0.001$, $F = 6.088$, $d.f. = 3.7$),

and total dyskinesias ($p < 0.001$, $F = 12.862$, $d.f. = 3.174$; fig. 2).

When compared with those before illumination (LID5), optical inhibition (LIGHT2) significantly decreased the AIM scores in the NpHR+590nm group: limb dyskinesia ($p = 0.006$), axial dyskinesia ($p < 0.001$), oral dyskinesia ($p = 0.004$), and total dyskinesias ($p < 0.001$). By contrast, the AIM scores in the NpHR+Sham group showed no significant changes, and the YFP+590nm group showed increases in limb, axial, and total dyskinesias (fig. 3).

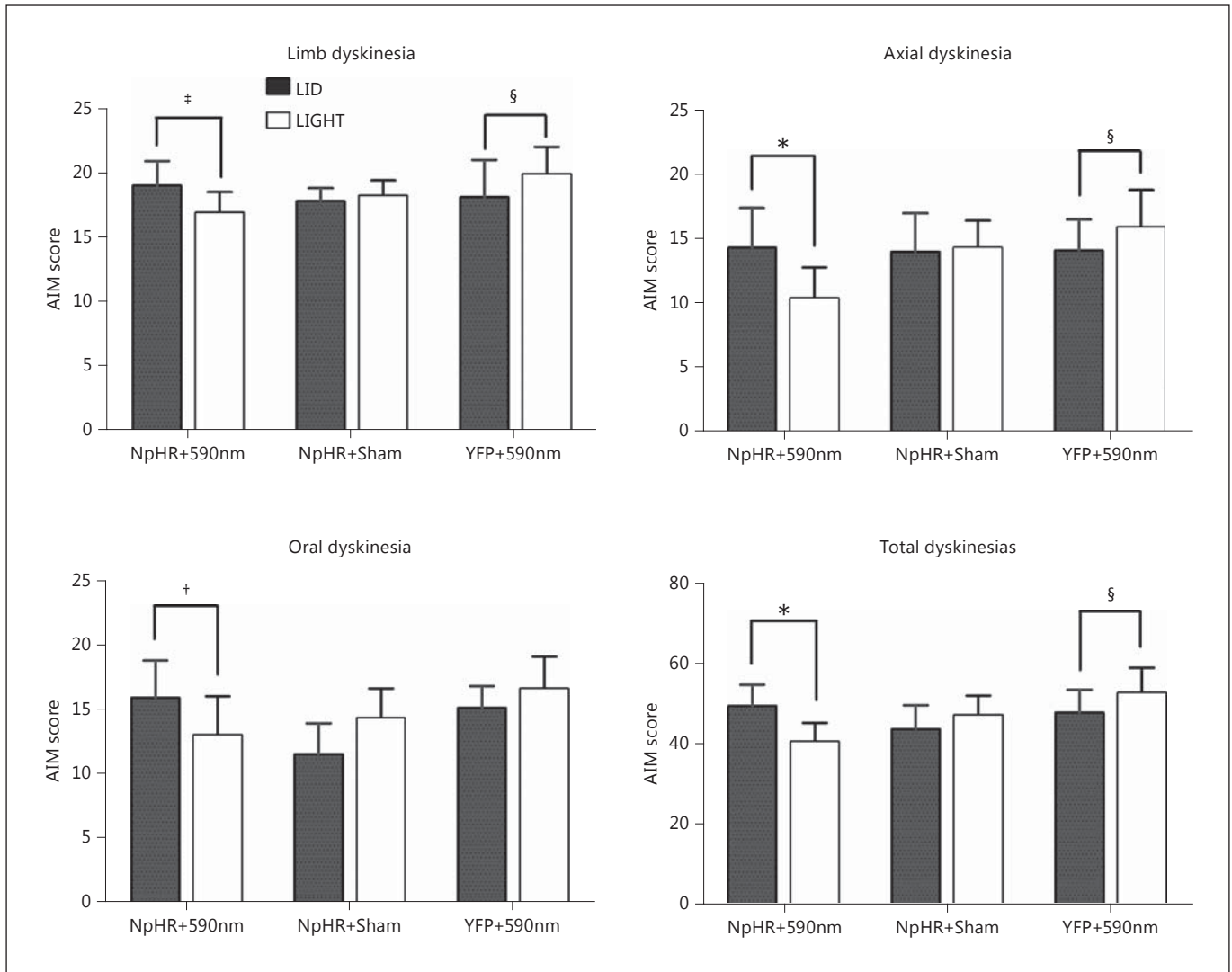


Fig. 3. Optical inhibition of the STN affects LID. Data are presented as the sum of the AIM scores during the observation time (120 min) in LID5 and LIGHT2 conditions. AIM scores in the NpHR+590nm group are significantly decreased (* $p < 0.001$,

$^\dagger p = 0.004$, and $^\ddagger p = 0.006$). By contrast, the NpHR+Sham group shows slight increases, and the YFP+590nm group shows significant increases in limb, axial, and total dyskinesias ($^\S p < 0.05$, paired t test).

Effect of Optical Inhibition of STN on the Severity of LID

The time courses for changes in limb, axial, oral, and total dyskinesias between the LID5 and LIGHT2 sessions were analyzed in the NpHR+590nm group (fig. 4). The results showed that there was no change in the peak severity of limb and oral LIDs until 60 min of light illumination (peak point of LID), but after this peak point, the scores for limb and oral dyskinesias decreased significantly under light illumination ($p < 0.05$; fig. 4). For axial dyskinesia scores, the rats showed significant decreases in the be-

ginning and for the overall time course of light illumination ($p < 0.05$; fig. 4). Therefore, the results revealed that optical inhibition of the STN affected the severity as well as the duration of axial dyskinesia, while it affected only the duration of limb and oral dyskinesias.

Effect of LID and Optical Inhibition of STN on Motor Activity

Before the L-DOPA injections began, the results of stepping tests showed that all animals in the NpHR+590nm, NpHR+Sham, and YFP+590nm groups had

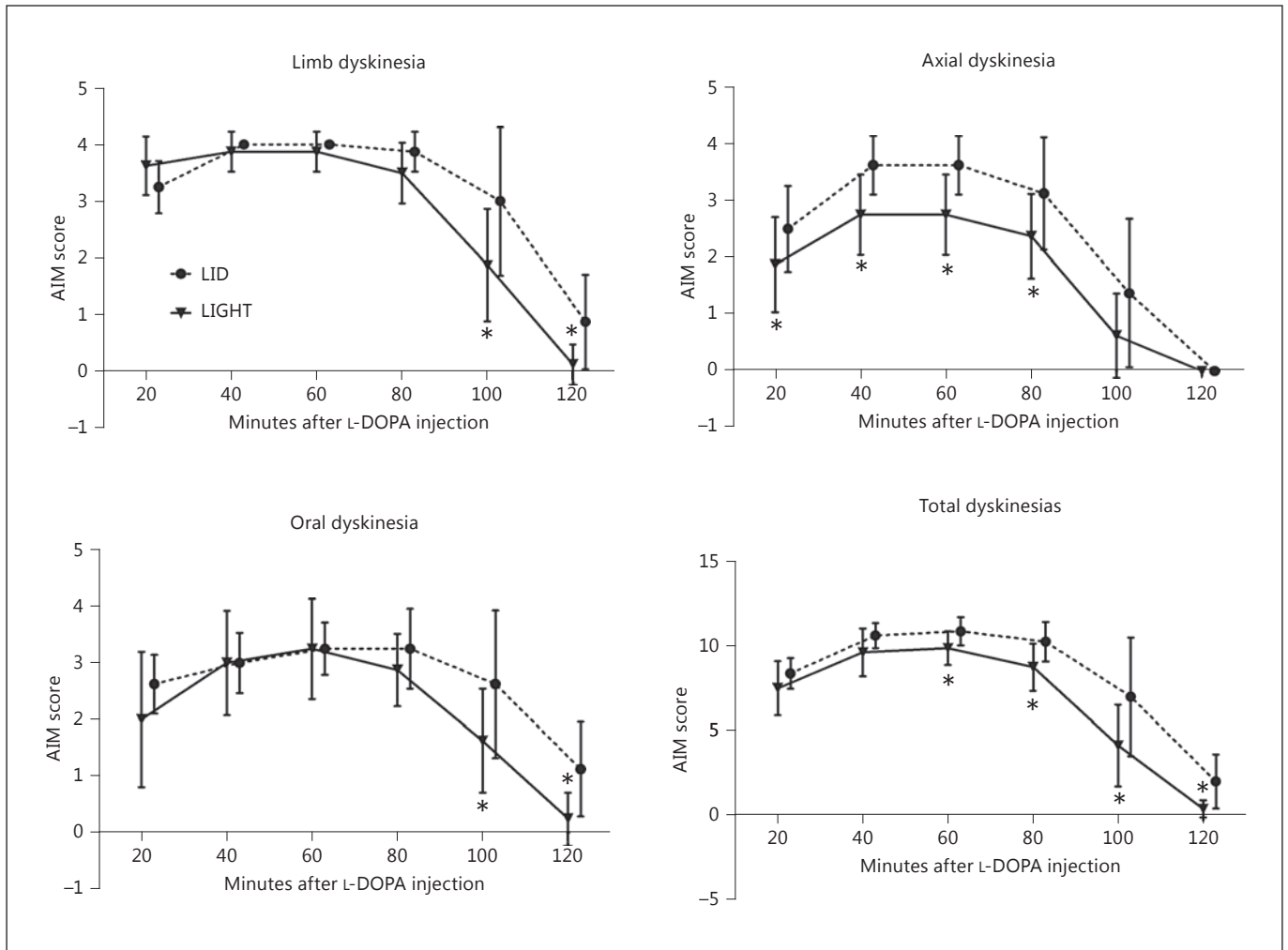


Fig. 4. Effect of optical inhibition of the STN on the severity of LID. The time course of limb, axial, oral, and total dyskinesias between LID5 and LIGHT2 sessions was compared in the NpHR+590nm group. There are significant decreases in limb, axial, oral, and total

dyskinesias under light illumination (590 nm; * $p < 0.05$, paired t test). The optical inhibition of the STN is effective for shortening the duration of all subtypes of dyskinesias, and the peak severity is also reduced in the axial dyskinesias.

contralateral forelimb akinesia induced by the 6-OHDA unilateral injection (PD state; fig. 5). The forehand and backward directions were more severe than the backhand direction for the contralateral forelimb akinesia in the PD state. During the first week of L-DOPA injections, the performance of the contralateral forelimb on stepping tests was significantly improved in all directions for all groups, while the performance of the ipsilateral forelimb worsened in all directions for all groups. Expectedly, the prolonged administration of L-DOPA induced a continuous decrease in contralateral forelimb touches in every group and every direction (LID1, LID2, and LID3; fig. 5). The prolonged administration of L-DOPA also induced a

continuous decrease in ipsilateral (intact) forelimb touches in every group and every direction (LID1, LID2, and LID3; fig. 5). Interestingly, there was a significant difference in the performance of ipsilateral forelimb in backhand direction induced by light stimulation across groups ($p = 0.38$, $F = 3.958$, $d.f. = 2$; fig. 5).

In the cylinder test, all rats in all groups showed marked motor deficits in the use of their contralateral forelimbs induced by the unilateral 6-OHDA injections in the Parkinson's disease model. After daily injections of L-DOPA, the contralateral forelimb touch rate was significantly increased in all groups, but all rats showed asymmetrical contralateral forelimb use. This asymmetry in forelimb

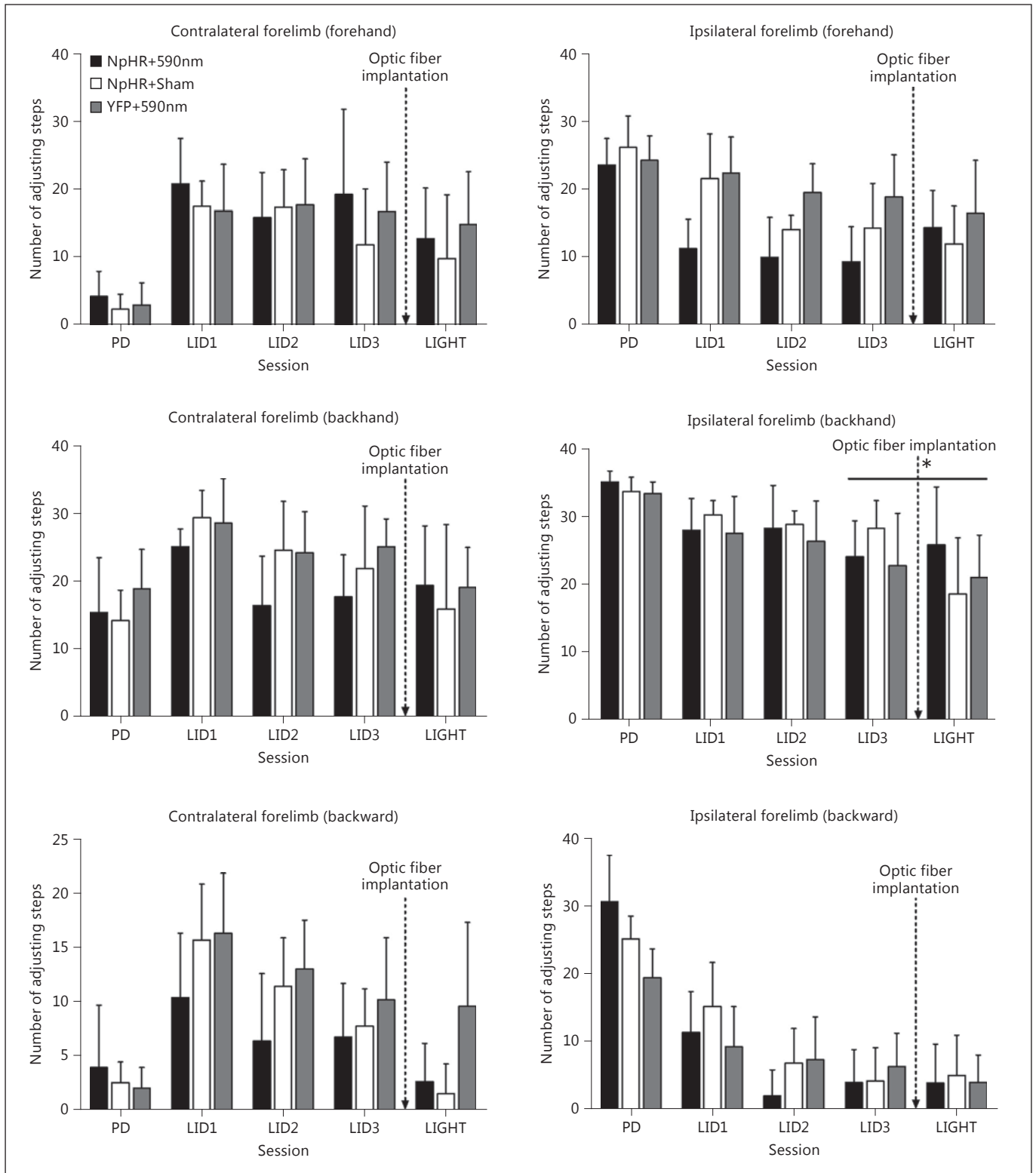


Fig. 5. Stepping tests examining three directions of movement for each forelimb. The tests were performed before L-DOPA injections (PD), once a week during L-DOPA injections (LID1, LID2, and LID3), and once with L-DOPA injections under light illumina-

tion (LIGHT). Data are shown as the number of forelimb touches. The ipsilateral forelimb (backhand) result showed significant difference across groups (* $p = 0.38$, $F = 3.958$, $d.f. = 2$; one-way ANOVA with Tukey's post hoc test).

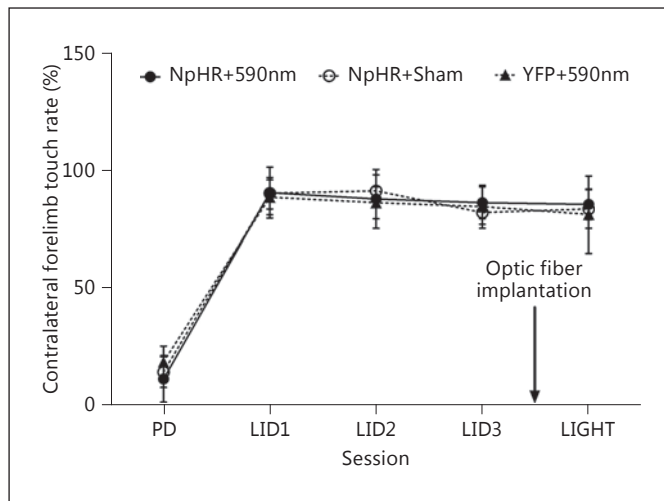


Fig. 6. Results of cylinder tests. The cylinder tests were performed before any L-DOPA injection (PD), once a week during L-DOPA injections (LID1, LID2, and LID3), and once with L-DOPA injections under light illumination (LIGHT). Data are shown as the percentage of contralateral forelimb contacts of both forelimb contacts. Light effect showed no significant difference across groups (one-way ANOVA with Tukey's post hoc test).

use persisted during the prolonged administration of L-DOPA (LID1, LID2, and LID3) and was not affected by light stimulation (LIGHT; fig. 6).

Histology

The results of confocal imaging showed that NpHR-YFP- and YFP-expressing cells in all groups were observed largely within the STN (fig. 7). The tip of the optic fiber was restricted to areas within the STN. Immunofluorescence for VGLUT2 revealed that the majority of YFP-expressing cells were VGLUT2-positive in all groups (fig. 7).

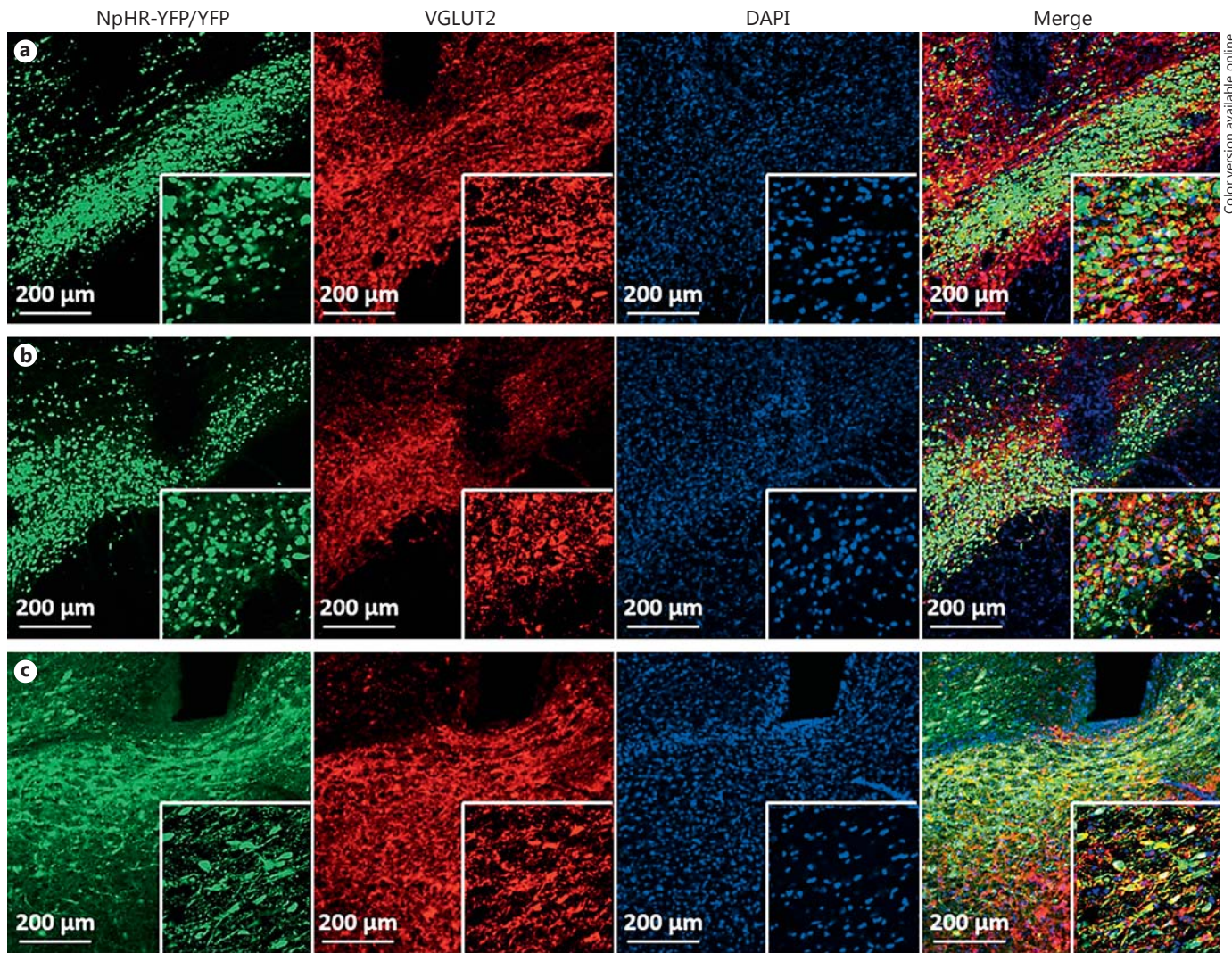
The SN sections in all groups showed considerable loss of TH-positive cells throughout the lesioned area (NpHR+590nm: $93.4 \pm 0.7\%$, NpHR+Sham: $93.1 \pm 4.0\%$, and YFP+590nm: $95.6 \pm 1.6\%$; fig. 8), indicating that the animals used in the present study had complete lesions.

Discussion

In this study, we tested the effect of optical inhibition of the STN on LID in a rat model of Parkinson's disease. Electrical DBS improves LID and reduces the need for medication in Parkinson's disease [24, 25]. However, the therapeutic mechanisms underlying DBS are unclear [6,

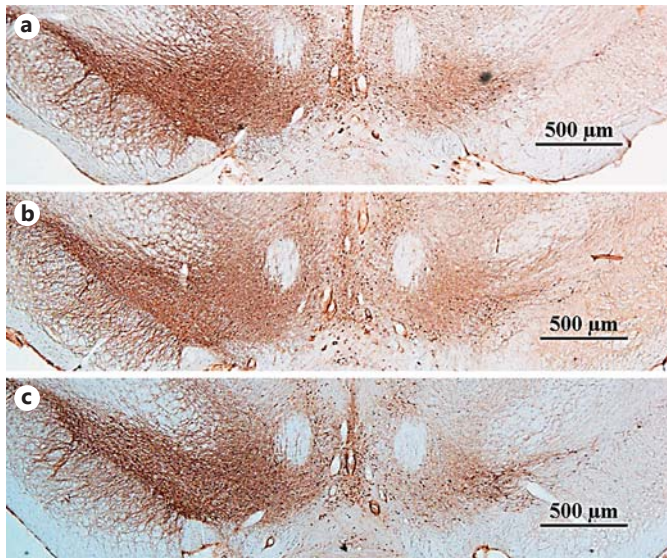
7]. Some researchers suggest that DBS appears to inhibit adjacent neurons because the therapeutic effects of DBS on Parkinson's disease are similar to those of lesions produced in the target areas [26]. Others suggest that STN DBS increases pallidal firing rates [7]. The therapeutic mechanisms of LID are difficult to explore because of the nature of this nonspecific electrical stimulation. Electrical DBS has some disadvantages, including an incompatibility with high-tesla MRI [27], the impossibility of simultaneous EEG, and the side effects from nonspecific electrical tissue stimulation [28]. To circumvent these complications associated with electrical DBS, there is a growing interest in optogenetic techniques that control the activity of specific target neurons and use metal-free materials, especially because 50% of the patients with Parkinson's disease receiving L-DOPA treatment develop LIDs within 5 years [29], and dyskinesias are the major motor symptoms treated with electrical DBS. In some aspects, there is concern that the results of low-frequency optical stimulation cannot be compared to those achieved with high-frequency electrical DBS, but we focused on the hypothesis that high-frequency DBS inhibits STN neurons, so high-frequency DBS was mimicked by optical inhibition. We used low-frequency (5 Hz) optic stimulation, which results in neuronal inhibition by suppressive function of halorhodopsin. 5 Hz was reported as the best parameter in a previous paper [30]. Thus, we considered that low-frequency optical stimulation could be comparable with high-frequency DBS in terms of neuronal inhibition. In a previous study, we demonstrated the therapeutic effect of STN inhibition on akinesia symptoms using optogenetics in a 6-OHDA-induced rat model of Parkinson's disease [12]. In the present study, we observed the therapeutic effects of optical STN inhibition on LIDs in a rat model of Parkinson's disease.

LID is associated with excessive glutamatergic transmission [15], and abnormal hyperactivity of STN neurons may also be related to dyskinesias because LID is produced in the presence of the hyperactive STN. The STN, which plays a critical role in the glutamate transmission regulating basal ganglia functions, is used as the most common target of electrical DBS in patients with Parkinson's disease [31]. Many studies using STN inhibition have been performed in patients or animal models of Parkinson's disease to evaluate the pathophysiology of LID [13, 24, 25, 32]. However, these inhibitory effects on the STN were generated using relatively nonselective electrical stimulation or a diffuse permanent lesion created with a toxin; therefore, the results may have led to inaccurate conclusions regarding the mechanism of therapeutic ac-



Color version available online

Fig. 7. Confocal images of NpHR-YFP and YFP-expressing cells. NpHR-YFP [NpHR+590nm group (a) and NpHR+Sham group (b)] and YFP [YFP+590nm group (c)] are expressed in the target of the STN. Cells positive for the glutamatergic marker VGLUT2 (red) are overlaid with NpHR-YFP (green) and YFP (green) expression. Magnification: 100× and 400× (lower right). **d** Tiled image of 100× magnification. A dotted circle represents the STN target. IC = Internal capsule; ZI = zona incerta. Colors refer to the online version only.



Color version available online

Fig. 8. TH-positive cell loss in the SN: NpHR+590nm group (a), NpHR+Sham group (b), and YFP+590nm (c). All groups show >90% loss of TH-positive cells in the lesioned site compared with the intact site.

tion. Here, we performed a more selective and transient inhibition of the STN using optogenetics *in vivo*. The optogenetics technique enables precise and transient control of specific target neurons using optogenetic expression and light illumination. There are two types of optogenetic actuators: inhibitory and excitatory. NpHR is a membrane protein that pumps chloride ions inward when illuminated with yellow light (590 nm) to inhibit action potentials, whereas channelrhodopsin is a cation channel that increases neuronal firing rates when illuminated with blue light (470 nm) [11, 30, 33]. Therefore, in this study, NpHR was selected to inhibit STN neurons. With respect to selectivity, the expression of the optogenetically installed AAV is driven by the specific combination of promoters used. The hSynapsin1 promoter used in the present study has been previously used to express optogenes in neurons to the exclusion of glial cells [33–36]. The usage of this promoter has the limitation that it may be taken up by either excitatory or inhibitory neurons [35]. Therefore, to increase selectivity, we stereotaxically injected the AAV only into the STN, which is confirmed in figure 7. The restricted illumination range, which loses 90% of its energy beyond 0.5 mm, reinforces the selectivity of optical STN inactivation [33].

By scoring AIMs, we found that the optical inhibition of the STN alleviated LID in a 6-OHDA rat model of Par-

kinson's disease. During optical inhibition of the STN, the NpHR+590nm group showed a decreased sum score during the observation time (120 min) for each dyskinesia subtype, whereas the animals in the other groups showed either no change or a slight increase in their sum scores (fig. 2, 3). Statistical results in the linear model and Greenhouse-Geisser correction of RM-ANOVA showed significant differences between groups (fig. 2). These results indicate that the transient inactivation of glutamatergic neurons in the STN by optical inhibition was effective for reducing LID. Interestingly, the dyskinesia scores in the YFP+590nm group actually increased under light illumination (fig. 3). This increase might have resulted from the exacerbation of dyskinesias by prolonged L-DOPA treatment, not from sensitization by light, because AIM scores in the NpHR+Sham group also showed a slight increase in a time-dependent pattern. The results from examining the time course of dyskinesias in the NpHR+590nm group revealed that optical inhibition of the STN was effective for shortening the duration of all subtypes of dyskinesias, and the peak severity was also reduced for axial dyskinesia (fig. 4). These findings suggest that acute optical inactivation of the STN induces a rapid attenuation of the dysregulated dopaminergic signaling. Whether inhibition of the STN by repeated light stimulation before L-DOPA administration affects the generation of LID should be studied in the future. In this animal model, axial dyskinesia is the main manifestation of dyskinesia because a PD rat model is unilateral. We consider that axial dyskinesia dominant improvement might be related to the topographical volume of motor area in the STN because STN neurons topographically innervate the sensory-motor area of cerebral cortex in rats [37]. The phenomenon that the second trial showed more improvement might be explained by the sensitization effect of halorhodopsin which was stimulated for a long time (2 h) in the first stimulation. Even in the first light-on condition, we could find significant differences in axial and total dyskinesias. Besides, we consider as a therapeutic effect that limb and oral dyskinesia scores showed no change or decrease in the NpHR±590nm group compared to increase in the two control groups. In this regard, two times of light-on tests are sufficient to demonstrate the optogenetic effect.

To evaluate forelimb motor activity, we conducted the stepping test and the cylinder test. The stepping test results revealed that the contralateral forelimb akinesia induced by 6-OHDA lesioning was initially improved by the L-DOPA treatment, but this therapeutic effect did not persist with prolonged L-DOPA treatments. Indeed, the ani-

mals in all groups reverted to the use of the contralateral forelimb in the backhand and backward directions, similar to that for animals in the Parkinson's disease model. This deterioration was not rescued by light stimulation. These results suggest that the antidyskinetic effect induced by optical inactivation of STN may not be adequately evaluated in the stepping test. Although dyskinesias developed following prolonged L-DOPA injections, there was a trend for improved motor activity of the contralateral forelimb compared with that for animals in the Parkinson's disease model. This improvement may have masked the antidyskinetic effect of the optical STN inhibition. Interestingly, the injection of L-DOPA induced a significant decrease in ipsilateral forelimb touches that were caused by axial dyskinesia in every direction for all groups compared with performances of animals in the Parkinson's disease model. The trend for improved performance of the ipsilateral forelimb in the stepping test after light illumination in the NpHR+590nm group supports our speculation that amelioration of axial LID by optical inactivation of the STN improved ipsilateral forelimb touches.

In the cylinder tests, the preference of all rats was changed from the use of the ipsilateral to the contralateral forelimb after L-DOPA injections. This change in forelimb preference was not affected by prolonged L-DOPA administration or light illumination, and increases in the use of the contralateral forelimb after L-DOPA injections persisted regardless of the increase in dyskinesias. The reason no improvement in LID was observed with optical inactivation might be that the preference in forelimb use was affected by the contralateral rotation and axial dyskinesia induced by LID, and the effect of optical inactivation was masked in the cylinder test.

The results of our histological study revealed that no damage was induced by the transient light illumination,

indicating that the potential lesion effect from the heat generated by the light energy was negligible. Figure 7 shows that NpHR-YFP or YFP was well-expressed and localized in the STN. The immunofluorescence for VGLUT2, a specific marker for glutamatergic neurons, revealed colocalization between YFP-expressing cells and VGLUT2-positive cells, indicating that NpHR-YFP or YFP was expressed in glutamatergic neurons of the STN (fig. 7). These findings suggest that the combination of the hSynapsin1 promoter and selective stereotactic injections provides appropriate control for the administration of optogenes. Figure 7 also shows that the tip of the inserted optic fiber was exclusively located in the STN.

Conclusions

We found that optical inactivation of the STN effectively reduces LID by shortening the duration of the LIDs as well as the severity of axial dyskinesia. In spite of showing the effects of optical inhibition in the STN, we need to investigate with electrophysiological study to provide more obvious evidence of the STN inhibition by optogenetics. Our results provide a useful foundation for future studies examining the optogenetic modulation of neural circuitry pertinent to Parkinson's disease treatment.

Acknowledgments

This work was supported by a 'KRCF National Agenda Project', by the Pioneer Research Center Program through the National Research Foundation of Korea funded by the Ministry of Science, ICT & Future Planning (NRF-2010-0019351), and by an Asan Life Science Institute Grant (12-241) from the Asan Medical Center, Seoul, Republic of Korea.

References

- 1 Hague S, Klaffke S, Bandmann O: Neurodegenerative disorders: Parkinson's disease and Huntington's disease. *J Neurol Neurosurg Psychiatry* 2005;76:1058–1063.
- 2 Hedlund E, Perlmann T: Neuronal cell replacement in Parkinson's disease. *J Intern Med* 2009;266:358–371.
- 3 de la Fuente-Fernández R, Schulzer M, Mak E, Calne DB, Stoessl AJ: Presynaptic mechanisms of motor fluctuations in Parkinson's disease: a probabilistic model. *Brain* 2004;127:888–899.
- 4 Benabid AL, Krack PP, Benazzouz A, Limousin P, Koudsie A, Pollak P: Deep brain stimulation of the subthalamic nucleus for Parkinson's disease: methodologic aspects and clinical criteria. *Neurology* 2000;55:S40–S44.
- 5 Fraix V, Pollak P, Van Blercom N, Xie J, Krack P, Koudsie A, Benabid A: Effect of subthalamic nucleus stimulation on levodopa-induced dyskinesia in Parkinson's disease. *Neurology* 2000;55:1921–1923.
- 6 Filali M, Hutchison WD, Palter VN, Lozano AM, Dostrovsky JO: Stimulation-induced inhibition of neuronal firing in human subthalamic nucleus. *Exp Brain Res* 2004;156:274–281.
- 7 Reese R, Leblois A, Steigerwald F, Pötter-Nerger M, Herzog J, Mehdorn HM, Deuschl G, Meissner WG, Volkmann J: Subthalamic deep brain stimulation increases pallidal firing rate and regularity. *Exp Neurol* 2011;229:517–521.
- 8 Gradinaru V, Mogri M, Thompson KR, Henderson JM, Deisseroth K: Optical deconstruction of parkinsonian neural circuitry. *Science* 2009;324:354–359.

- 9 Carter ME, de Lecea L: Optogenetic investigation of neural circuits in vivo. *Trends Mol Med* 2011;17:197–206.
- 10 Deisseroth K, Feng G, Majewska AK, Miesenböck G, Ting A, Schnitzer MJ: Next-generation optical technologies for illuminating genetically targeted brain circuits. *J Neurosci* 2006;26:10380–10386.
- 11 Gradinaru V, Thompson KR, Zhang F, Mogri M, Kay K, Schneider MB, Deisseroth K: Targeting and readout strategies for fast optical neural control in vitro and in vivo. *J Neurosci* 2007;27:14231–14238.
- 12 Yoon HH, Park JH, Kim YH, Min J, Hwang E, Lee CJ, Suh J-KF, Hwang O, Jeon SR: Optogenetic inactivation of the subthalamic nucleus improves forelimb akinesia in a rat model of Parkinson disease. *Neurosurgery* 2014;74:533–541.
- 13 Aristieta A, Azkona G, Sagarduy A, Miguez C, Ruiz-Ortega JA, Sanchez-Pernaute R, Ugedo L: The role of the subthalamic nucleus in L-DOPA induced dyskinesia in 6-hydroxydopamine lesioned rats. *PLoS One* 2012;7:e42652.
- 14 Wichmann T, Dostrovsky JO: Pathological basal ganglia activity in movement disorders. *Neuroscience* 2011;198:232–244.
- 15 Sgambato-Faure V, Cenci MA: Glutamatergic mechanisms in the dyskinesias induced by pharmacological dopamine replacement and deep brain stimulation for the treatment of Parkinson's disease. *Prog Neurobiol* 2012;96:69–86.
- 16 Kollensperger M, Stefanova N, Pallua A, Puschban Z, Dechant G, Hainzer M, Reindl M, Poewe W, Ninkhah G, Wenning GK: Striatal transplantation in a rodent model of multiple system atrophy: effects on L-Dopa response. *J Neurosci Res* 2009;87:1679–1685.
- 17 Salin P, Manrique C, Forni C, Kerkerian-Le Goff L: High-frequency stimulation of the subthalamic nucleus selectively reverses dopamine denervation-induced cellular defects in the output structures of the basal ganglia in the rat. *J Neurosci* 2002;22:5137–5148.
- 18 Navailles S, Benazzouz A, Bioulac B, Gross C, Deurwaerdere P: High-frequency stimulation of the subthalamic nucleus and L-3,4-dihydroxyphenylalanine inhibit in vivo serotonin release in the prefrontal cortex and hippocampus in a rat model of Parkinson's disease. *J Neurosci* 2010;30:2356–2364.
- 19 Lee CS, Cenci MA, Schulzer M, Bjorklund A: Embryonic ventral mesencephalic grafts improve levodopa-induced dyskinesia in a rat model of Parkinson's disease. *Brain* 2000;123:1365–1379.
- 20 Lundblad M, Andersson M, Winkler C, Kirik D, Wierup N, Cenci MA: Pharmacological validation of behavioural measures of akinesia and dyskinesia in a rat model of Parkinson's disease. *Eur J Neurosci* 2002;15:120–132.
- 21 Paille V, Henry V, Lescaudron L, Brachet P, Damier P: Rat model of Parkinson's disease with bilateral motor abnormalities, reversible with levodopa, and dyskinesias. *Mov Disord* 2007;22:533–539.
- 22 Schallert T, Fleming SM, Leasure JL, Tillerson JL, Bland ST: CNS plasticity and assessment of forelimb sensorimotor outcome in unilateral rat models of stroke, cortical ablation, parkinsonism and spinal cord injury. *Neuropharmacology* 2000;39:777–787.
- 23 Hwang O, Baker H, Gross S, Joh TH: Localization of GTP cyclohydrolase in monoaminergic but not nitric oxide-producing cells. *Synapse* 1998;28:140–153.
- 24 Oueslati A, Sgambato-Faure V, Melon C, Kachidian P, Gubellini P, Amri M, Kerkerian-Le Goff L, Salin P: High-frequency stimulation of the subthalamic nucleus potentiates L-DOPA-induced neurochemical changes in the striatum in a rat model of Parkinson's disease. *J Neurosci* 2007;27:2377–2386.
- 25 Russmann H, Ghika J, Combremont P, Villemeure J, Bogousslavsky J, Burkhard P, Vingerhoets F: L-dopa-induced dyskinesia improvement after STN-DBS depends upon medication reduction. *Neurology* 2004;63:153–155.
- 26 Chiken S, Nambu A: Disrupting neuronal transmission: mechanism of DBS? *Front Syst Neurosci* 2014;8:33.
- 27 Oluigbo CO, Rezai AR: Magnetic resonance imaging safety of deep brain stimulator devices. *Handb Clin Neurol* 2013;116:73–76.
- 28 Aravanis AM, Wang LP, Zhang F, Meltzer LA, Mogri MZ, Schneider MB, Deisseroth K: An optical neural interface: in vivo control of rodent motor cortex with integrated fiberoptic and optogenetic technology. *J Neural Eng* 2007;4:S143–S156.
- 29 Tambasco N, Simoni S, Marsili E, Sacchini E, Murasecco D, Cardaioli G, Rossi A, Calabresi P: Clinical aspects and management of levodopa-induced dyskinesia. *Parkinsons Dis* 2012;2012:745947.
- 30 Zhang F, Wang LP, Brauner M, Liewald JF, Kay K, Watzke N, Wood PG, Bamberg E, Nagel G, Gottschalk A, Deisseroth K: Multimodal fast optical interrogation of neural circuitry. *Nature* 2007;446:633–639.
- 31 Porter R, Greene JG, Higgins D, Greenamyre JT: Polysynaptic regulation of glutamate receptors and mitochondrial enzyme activities in the basal ganglia of rats with unilateral dopamine depletion. *J Neurosci* 1994;14:7192–7199.
- 32 Marin C, Bonastre M, Mengod G, Cortés R, Rodríguez-Oroz MC, Obeso J: Subthalamic 6-OHDA-induced lesion attenuates levodopa-induced dyskinesias in the rat model of Parkinson's disease. *Exp Neurol* 2013;250:304–312.
- 33 Yizhar O, Fenno LE, Davidson TJ, Mogri M, Deisseroth K: Optogenetics in neural systems. *Neuron* 2011;71:9–34.
- 34 Diester I, Kaufman MT, Mogri M, Pashaie R, Goo W, Yizhar O, Ramakrishnan C, Deisseroth K, Shenoy KV: An optogenetic toolbox designed for primates. *Nat Neurosci* 2011;14:387–397.
- 35 Nathanson JL, Yanagawa Y, Obata K, Callaway EM: Preferential labeling of inhibitory and excitatory cortical neurons by endogenous tropism of adeno-associated virus and lentivirus vectors. *Neuroscience* 2009;161:441–450.
- 36 Kügler S, Kilic E, Bähr M: Human synapsin 1 gene promoter confers highly neuron-specific long-term transgene expression from an adenoviral vector in the adult rat brain depending on the transduced area. *Gene Ther* 2003;10:337–347.
- 37 Degos B, Deniau JM, Le Cam J, Mailly P, Maurice N: Evidence for a direct subthalamocortical loop circuit in the rat. *Eur J Neurosci* 2008;27:2599–2610.